TRAMS: A new dynamic cloud model for Titan's methane clouds

Erika L. Barth[1] and Scot C. R. Rafkin[1]

Received 1 November 2006; revised 6 December 2006; accepted 5 January 2007; published 10 February 2007.

[1] Convective clouds on Titan may play an important role in climate dynamics, atmospheric chemistry, and the overall volatile cycle. To study the formation and evolution of these clouds, we have developed the Titan Regional Atmospheric Modeling System (TRAMS). TRAMS is a three-dimensional, time-dependent, coupled fully compressible dynamic and microphysical model capable of simulating methane and ethane clouds in Titan's atmosphere. In initial model tests over a two-dimensional domain, a warm bubble or random temperature perturbations trigger a parcel of air to rise. For an initial methane profile with a 60% surface humidity, convection occurs for positive temperature perturbations of 1 K or greater. Cloud tops are between 25 and 35 km, consistent with observations of the south polar clouds. For a drier methane environment in the lower atmosphere, characteristic of the Huygens landing site, convection does not occur, but a layer of stratiform clouds is able to form at altitudes around 10 km. **Citation:** Barth, E. L., and S. C. R. Rafkin (2007), TRAMS: A new dynamic cloud model for Titan's methane clouds, *Geophys. Res. Lett.*, *34*, L03203, doi:10.1029/2006GL028652.

1. Introduction

[2] Titan's polar clouds have been a prominent feature in the southern hemisphere for a number of years. Clouds were initially detected through brightness changes across Titan's disk [*Griffith et al.*, 1998, 2000] and later, with improvements in adaptive optics, imaged through ground-based observing [*Roe et al.*, 2002; *Brown et al.*, 2002]. The Cassini spacecraft and long-term ground-based observations [*Schaller et al.*, 2006] have shown a recent drop in occurrence of these south pole clouds, possibly linked to seasonal changes.

[3] *Griffith et al.* [2000] argued the clouds they detected were convective in nature due to rapid lifetimes (hours) and common heights ($\sim$25 km). For convective clouds to form, a parcel of moist air must rise until reaching saturation at the lifting condensation level (LCL). Further upward forcing of the parcel results in condensation and latent heat release and the parcel will cool at the saturated adiabatic lapse rate. If the environmental lapse rate exceeds the saturated adiabatic lapse rate, and the parcel continues to rise, it will reach a level at which it becomes buoyant relative to its surroundings, the level of free convection (LFC). The parcel can then freely accelerate upwards. *Griffith et al.* [2000] looked into the stability of Titan's atmosphere and found an LCL of 2 km and an LFC of 5.5 km for a humidity of 60% at the surface; the LFC is lowered to 2 km for a parcel at 80% humidity.

[4] *Awal and Lunine* [1994] focused on local convective processes; Voyager only saw the lapse rate in two locations, hence a low probability of being in the region of localized vigorous convection. For surface methane volume mixing ratios within Voyager data error bars (3–7%), they found the areal coverage of moist plumes to be at most 10^{-5}, but more likely $\sim 10^{-7}$. Plume velocities resulting in moist convection were $\sim$1–10 m/s depending on surface methane and the environment relative humidity at the parcel's saturation point.

[5] A recent convection model by *Hueso and Sánchez-Lavega* [2006] also found strong updrafts of 1–20 m/s are necessary to initiate convection. They developed a 3-D methane convection model to characterize the amount of precipitation produced by storms (composed of methane droplets) at Titan's South Pole. For methane humidities in the troposphere greater than 80%, they could produce vigorous methane storms which dissipated in 5–8 hrs and left behind more than 100 kg/m^2 of methane rainfall on the surface.

[6] There are a number of differences between our model and that of *Hueso and Sánchez-Lavega* [2006]. They employ a different dynamical core which uses the anelastic approximation to the continuity equation. Our model is fully compressible; also we include additional microphysical processes such as nucleation, freezing and melting and a more rigorous treatment of the coalescence of cloud particles as described in Section 2. Nevertheless, we include some comparisons between our model results and theirs in Section 3.

2. Modeling

[7] The Regional Atmospheric Modeling System (RAMS) was developed at Colorado State University in the mid-1980s. The model is a fusion of several terrestrial weather simulation codes [*Mahrer and Pielke*, 1977; *Tripoli and Cotton*, 1982; *Tremback and Kessler*, 1985; *Pielke et al.*, 1992] and has been successfully adapted to study the weather on Mars [*Rafkin et al.*, 2001]. RAMS is a fully compressible non-hydrostatic model, which permits the simulation of atmospheric flows with large vertical accelerations, such as convective clouds. The model is three-dimensional, time-dependent, and easily configured over a wide range of user-specified horizontal grid spacings that can range from meters to hundreds of kilometers. The vertical coordinate is a terrain-influenced sigma system that may be geometrically stretched with height to provide highest resolution in the boundary layer.

[8] A coupled dynamic and microphysics model, Titan-RAMS (TRAMS), was adapted from RAMS to simulate clouds on Titan. We run the model in 2-D, with 55 to 60 vertical layers up to 50 km and 200 to 400 horizontal layers of 1 km spacing. Vertical grid spacing is 10 s of meters near

[1]Southwest Research Institute, Boulder, Colorado, USA.

0094-8276/07/2006GL028652$05.00

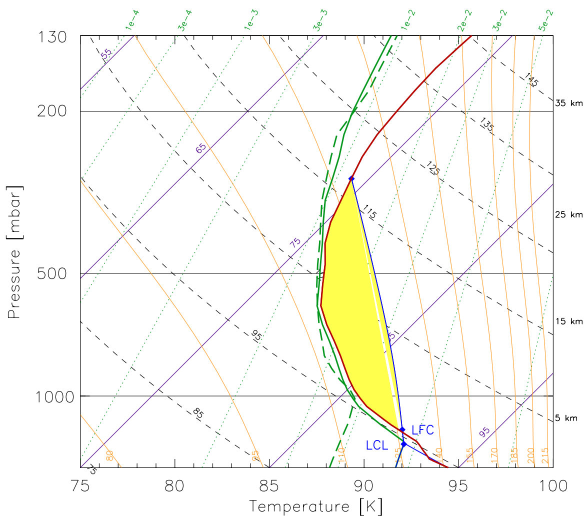

Figure 1. Methane "soundings" in Titan's troposphere on a skew T log P diagram. The solid red line represents the *Lellouch et al.* [1989] temperature profile. The solid green line is a hypothetical methane profile based on *Lellouch et al.* [1989], while the dashed green line is the Huygens probe methane measurement given by *Niemann et al.* [2005]. Other lines are: isobars (solid black), isotherms (solid purple), adiabats (dashed black), moist adiabats (solid orange), and constant mixing ratios (dotted green). The blue lines indicate the state of a parcel lifted from the surface (assuming the *Lellouch et al.* [1989] methane) as described in the text. The vapor pressure equation used in constructing the diagram is for a liquid methane-nitrogen mixture near the surface and methane ice above the freezing point of the mixture. The Convective Available Potential Energy (CAPE) for the Lellouch "sounding" is shaded in yellow. The *Niemann et al.* [2005] profile has only a small amount of CAPE between 11 and 19 km.

the surface up to 2 km layers aloft. The microphysics includes processes for haze particles (coagulation, sedimentation) and cloud particles (nucleation, condensation, coalescence, sedimentation, evaporation), for a number of size bins. *Barth and Toon* [2003, 2006] describes the equations governing the microphysics package.

[9] The haze particles range in size from 13 Å to 3.35 μm (bin-center radius). Cloud particles overlap the haze population at 0.04 μm and extend to 5 mm size; droplets growing any larger would be subject to breakup. The number of bins for each particle type depends on the mass ratio between bins; simulations reported here use a ratio of 8.

[10] The model is initialized uniformly in the x-direction from the temperature/density profiles of *Lellouch and Hunten* [1987]. Haze particles are initialized and added with a flux at the top boundary following [*Barth and Toon*, 2003]. Several methane profiles are explored, including [*Lellouch et al.*, 1989], the Huygens landing site sounding [*Niemann et al.*, 2005], combinations of the two, and cases with higher surface humidities. Figure 1 shows two simulated "*soundings*" on a *skew T log P* thermodynamic diagram. Soundings are commonly used to determine atmospheric stability with respect to moist convection and cloud properties in a given environment. Unsaturated parcels follow an adiabat and constant (CH_4-N_2) mixing ratio line. Once saturated, the parcel follows the moist adiabat. Stability is determined by comparing parcel temperature to that of the environment at any given level. In each plotted sounding, a parcel at the surface is unsaturated and colder than the environment when initially lifted. Forced lifting allows for condensation at the lifting condensation level (LCL). With further forced lifting, the parcel becomes warmer than the environment at the level of free convection (LFC). The total integrated temperature difference (area between the parcel and environment temperature curves) is the convective available potential energy (CAPE). A trigger is needed to provide energy for the parcel to reach the LFC. For the Lellouch case, the LCL is close in altitude to the LFC (LCL at 2.7 km, LFC at 4.3 km) and there is ~915 J/kg of CAPE to drive convection. The *Niemann et al.* [2005] sounding has only about 60 J/kg of CAPE and requires lifting the parcel higher (6 km LCL, 11 km LFC), and so is not conducive to convective clouds (The *Fulchignoni et al.* [2005] temperature profile, at most 1 K lower near the surface, moves the LFC closer to 7 km, but still results in the same order magnitude of CAPE). Stratiform clouds above 1000 mbar, where the parcel is near saturation, are possible.

[11] The TRAMS microphysics package forms clouds of various compositions: ethane ice, methane ice, methane droplet (where methane vapor pressure and melting temperature are altered through dissolved N_2 as described by *Thompson et al.* [1992]), and mixed methane/ethane clouds. All have a tholin haze particle as a cloud condensation nuclei (CCN). Here we neglect ethane and look only at simulations of methane droplet and ice clouds. Nucleation follows the classical theory as in work by *Pruppacher and Klett* [1997]. The contact parameter for methane is 0.981 (critical saturation of 1.10 (D. B. Curtis et al., personal communication, 2005)).

3. Results and Discussion

[12] A warm bubble at the surface forces the air parcel to rise. The bubble has a gaussian shape (σ = 4), vertical size of 200 m, and is centered in x. The bubble is perhaps representative of forcing from sensible heat flux, but is not meant to quantify the amount of energy which can reach Titan's surface.

3.1. Convective Clouds

[13] With the *Lellouch et al.* [1989] methane profile (60% surface humidity for pure liquid methane), 1 K bubbles are sufficient to lift the air parcel to the LFC and subsequent latent heating drives convective clouds. Cloud properties (e.g., number of particles, vertical extent, updraft velocities) are independent of bubble temperature; warmer bubbles merely expedite the time to initial condensation. The cloud top between 30 and 35 km is consistent with Figure 1 and cloud heights estimated from observations [e.g., *Griffith et al.*, 2000]. Particle concentration is large (~1–10 cm^{-3}), with updrafts over 10–20 m/s (Figure 2). Such velocities are consistent with the plume model of *Awal and Lunine* [1994] and the convection model of *Hueso and Sánchez-Lavega* [2006]. Increasing the bubble spatial size produces clouds of similar physical properties. These clouds only

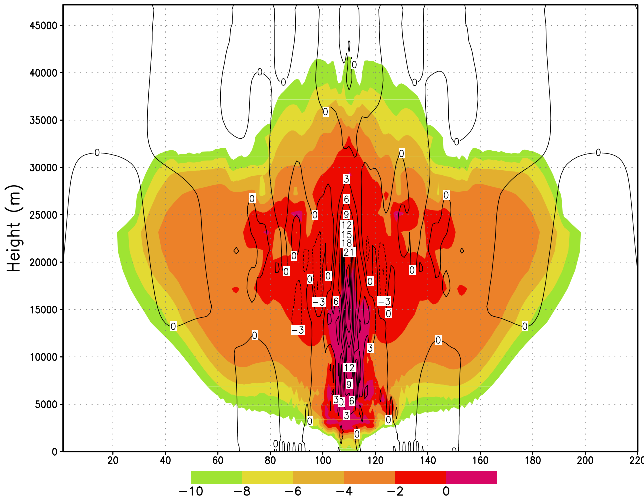

Figure 2. Convective cloud produced using the methane profile constructed from *Lellouch et al.* [1989], three hours after initial cloud formation. The lower portion of the cloud is composed of methane-nitrogen droplets. Above about 16 km, the particles are methane ice crystals. The shaded contours are $\log_{10}$ of the cloud particle number concentration (where N is per cubic centimeter). Contour lines indicate vertical velocity (m/s). Horizontal distance (x-axis) is kilometers.

differ in the timescales of cloud formation. The cloud is relatively independent of the bubble dimensions.

[14] The freezing point of a methane-nitrogen mixture occurs near 16 km altitude. Aside from the possibility of a supercooled methane mixture (which seems unlikely in light of Huygens observations, [e.g., *Tokano et al.*, 2006], methane will nucleate as ice crystals above this altitude. The convective clouds produced by TRAMS are composed of solid methane particles above 16 km and liquid methane-nitrogen droplets below (all with a haze particle core). Falling ice crystals melt at a rate of 100 s^{-1} and droplet particles carried aloft freeze at a rate of 10 s^{-1}. In the central part of the cloud, where nucleation is occurring, the average radius of cloud particles ranges from $\sim$10–20 μm. Upon freezing, the ice particles grow to $\sim$100–400 μm. Away from the center, the ice particles tend to be smaller in size than the droplets. Ice particle average radius is about 600 μm, while droplets are about 850 μm. A small number of droplets grow to 5 mm after a few hours.

[15] Haze particles are initialized uniformly in the x-direction, with an average radius of $\sim$0.2–0.3 μm. In regions where nucleation occurs, the average radius shifts to $\sim$0.01 μm, too small to serve as effective CCN. As cloud particles coalesce and later evaporate, they can create small regions where the average haze particle radius exceeds 0.5 μm.

3.2. Stratiform Clouds

[16] At the Huygens landing site, there is insufficient energy for convection. Instead, gravity waves triggered by the bubble produce layered (stratiform) clouds near the already saturated layer. Figure 3 shows clouds present near 10 km. Vertical velocities are generally under 10 cm/s. The abundance of cloud particles is much less than the convective clouds described above, however particle sizes are similar (mean radius of order 600 μm).

[17] This thin layer of stratiform clouds at the simulated Huygens landing site is consistent with DISR (Descent Imager/Spectral Radiometer) and GCMS (Gas Chromatograph Mass Spectrometer) data [*Tomasko et al.*, 2005; *Niemann et al.*, 2005], and analysis by *Tokano et al.* [2006]. They found an optically thin methane haze near 21 km and evidence for another distinct cloud layer below 16 km, the transition region for CH_4 ice and liquid CH_4-N_2. We cannot make the stratiform ice clouds with a warm bubble trigger in TRAMS, indicating other forcing mechanisms besides sensible heat flux driving the formation of the ice clouds (e.g., gravity waves, radiational cooling). The sounding shows such clouds could form if air is forced at 16 km, but these clouds will not be surface bound.

3.3. Rainfall

[18] The thin clouds at the Huygens landing site lack sufficient mass for significant methane rainfall. Even after 8 hours, the amount of methane precipitation at the surface in any given location is less than 10^{-8} kg/m^2. For the 60% surface humidity case (Lellouch model), the large amount of methane in the atmosphere prolongs the storms. The initial cloud has completely dissipated within 5 hours. As the cloud particles are raining out and evaporating near the cloud base, downdrafts produce pools of cold air, triggering additional cloud formation, and the cycle continues throughout the rest of the simulation.

[19] Figure 4 shows significant rain accumulation from the convective cloud, even for cases with less methane abundance (50 and 55% surface humidities). However, this is less than the precipitation predicted by *Hueso and Sánchez-Lavega* [2006]. The main difference is the droplet

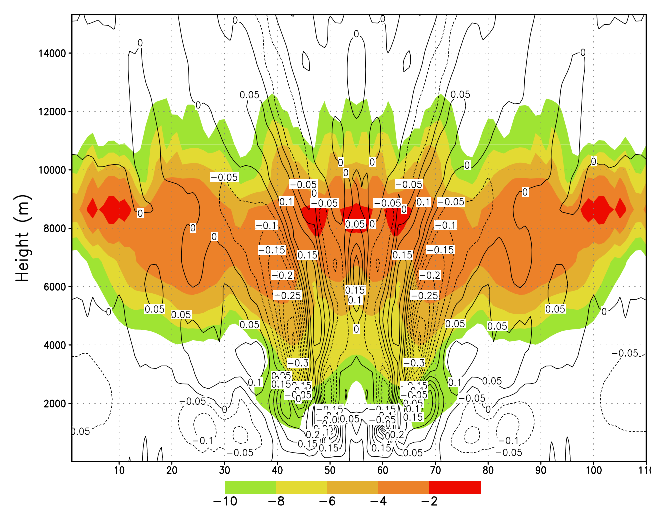

Figure 3. Stratiform cloud produced using the methane sounding from the Huygens landing site three hours after initial cloud formation. The cloud is composed entirely of methane-nitrogen droplets; no ice crystals are present. The shaded contours are $\log_{10}$ of the cloud particle number concentration (where N is per cubic centimeter). Contour lines indicate vertical velocity (m/s). Horizontal distance (x-axis) is in kilometers. Altitude is shown only up to 15 km as clouds do not form at higher altitudes for this case.

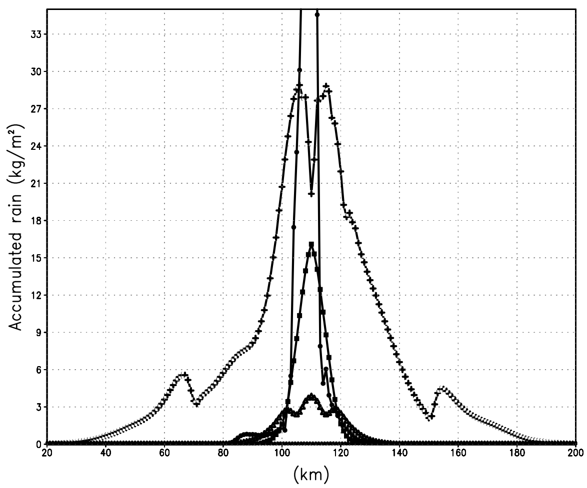

Figure 4. Accumulation of methane rain at the surface at a time of 5 hours after initiating cloud formation. Curves are shown for three different methane initializations (surface humidities): 60% (plus), 55% (squares), and 50% (triangles). In cases where the surface humidity is even greater (70% and 80%) the curves (not shown) are similar in appearance to the 60% curve, but peak at higher values (80 kg/m^2 and 130 kg/m^2, respectively). Also shown are curves for the 60% methane case with 100% coalescense efficiency (circles) and no coalescence (x). The peak in the 100% efficiency curve is about 80 kg/m^2. The no coalescence case has a maximum rain accumulation of about 0.005 kg/m^2. Multiplying the accumulated rain (in the given units) by a factor of 1/4 gives approximate centimeters of methane.

mass. *Hueso and Sánchez-Lavega* [2006] grow more droplets to 5 mm radius by assuming 100% efficiency, whereas the efficiencies for our coalescence kernels are a function of the colliding particle sizes [*Beard and Ochs*, 1984]. Efficiencies greater than 90% are generally only found for collisions between 80–100 μm particles. Uniformly increasing our efficiencies to 100% produces several hundred kg/m^2 rain accumulation.

3.4. Multiple Storms

[20] A single storm triggered by a warm bubble may not be representative of a broad convectively active environment because a single storm will neither compete with other storms for CAPE nor will it suffer from destructive compensating subsidence generated by neighboring storms. To explore these potential effects, we constructed a simulation 400 km in horizontal extent initialized with random temperature perturbations not to exceed 3 K in magnitude in the lowest few hundred meters superimposed on the Lellouch methane profile. This initialization procedure had the effect of triggering nearly simultaneously numerous convective cells. Using cyclic boundary conditions created an effectively infinite numerical domain such that no storm could escape the effects from its neighbors.

[21] The effect of storm competition is pronounced (Figure 5). While the number concentrations are similar to the convective clouds described in section 3.1, the horizontal extent of the cloud and in particular the cloud anvil is substantially reduced. Upper level storm outflow is impeded in these simulations; neighboring storm circulations interact. Also, the magnitude of the updrafts, typically 10–12 m/s, are ~1/2 of the isolated bubble case. The weaker updrafts further decrease the upper level storm outflow that is necessary to balance the updraft mass flux. As in the warm bubble cases, artificially increasing the coalescence efficiency to 100% vastly increases the surface precipitation. Still, even the standard coalescence formulation can produce upwards of 10 cm of surface precipitation.

[22] Storm life cycles are also markedly different. After one convective cycle, the atmosphere is nearly uniformly depleted of CAPE; no additional storms can develop. Images of Titan's south polar clouds clearly show numerous storms at any given time. Thus, these storms are likely to behave as the complex of storms simulated with random perturbations. However, the simulations indicate that energy for the storms is depleted within hours, suggesting an efficient convective destabilization mechanism to offset the stabilizing effects of the clouds. On Earth, convective energy is typically resupplied via large-scale circulations, allowing additional convective cycles. Perhaps Titan's large scale circulation does the same.

4. Summary

[23] We have developed a convection model for Titan with methane cloud microphysics and demonstrated its ability to produce clouds. While the clouds shown in these simulations are triggered by an artificial warm bubble or temperature perturbation, their characteristics are consistent with observations (e.g., cloud top height, large horizontal extent, short lifetimes). The simulations show that despite only small variation in Titan's temperature profile in the troposphere from equator to pole, the possibilities for convective clouds vary widely as this is tied to the methane profile. Moist environments of $\gtrsim$50% surface humidity produce strong convective storms with large updraft velocities while a dry environment like the Huygens landing site can only produce thin stratiform clouds. The appearance of clouds at the pole, if they are indeed convective, would then be evidence of a wetter environment than that observed by

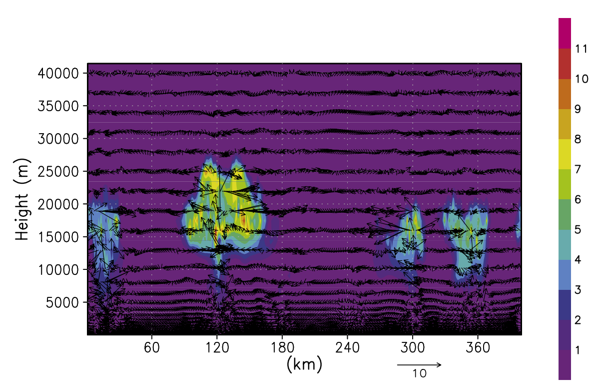

Figure 5. Multiple methane storms at 3 hours after initial cloud formation for a model initiated with random temperature perturbations. The shaded surfaces are mixing ratio of cloud particles (g/kg) and the black arrows show wind direction. The magnitude of the winds can be estimated from the 10 m/s arrow shown below the x-axis. Horizontal distances are in kilometers.

the Huygens probe. Future work will involve an analysis of plausible trigger mechanisms, including surface heating, topography and rising motions associated with Titan's Hadley circulation, and 3-D simulations with winds, as well as the effects of ethane in methane droplets, which is likely to play a significant role in the stability of raindrops near the surface.

[24] **Acknowledgments.** We thank Tim Michaels for useful input concerning development of the TRAMS code and Chris McKay and an anonymous reviewer for their helpful comments. This work was supported through an Internal Research and Development award at Southwest Research Institute and the NASA Planetary Atmospheres program.

References

Awal, M., and J. I. Lunine (1994), Moist convective clouds in Titan's atmosphere, *Geophys. Res. Lett.*, *21*, 2491–2494.

Barth, E. L., and O. B. Toon (2003), Microphysical modeling of ethane ice clouds in Titan's atmosphere, *Icarus*, *162*, 94–113, doi:10.1016/S0019-1035(02)00067-2.

Barth, E. L., and O. B. Toon (2006), Methane, ethane, and mixed clouds in Titan's atmosphere: Properties derived from microphysical modeling, *Icarus*, *182*, 230–250, doi:10.1016/j.icarus.2005.12.017.

Beard, K. V., and H. T. Ochs (1984), Collection and coalescence efficiencies for accretion, *J. Geophys. Res.*, *89*, 7165–7169.

Brown, M. E., A. H. Bouchez, and C. A. Griffith (2002), Direct detection of variable tropospheric clouds near Titan's south pole, *Nature*, *240*, 795–797, doi:10.1038/nature01302.

Fulchignoni, M., et al. (2005), In situ measurements of the physical characteristics of Titan's environment, *Nature*, *438*, 785–791, doi:10.1038/nature04314.

Griffith, C. A., T. Owen, G. A. Miller, and T. Geballe (1998), Transient clouds in Titan's lower atmosphere, *Nature*, *395*, 575–578, doi:10.1038/26920.

Griffith, C. A., J. L. Hall, and T. R. Geballe (2000), Detection of daily clouds on Titan, *Science*, *290*, 509–513.

Hueso, R., and A. Sánchez-Lavega (2006), Methane storms on Saturn's moon Titan, *Nature*, *442*, 428–431, doi:10.1038/nature04933.

Lellouch, E., and D. M. Hunten (1987), Titan atmosphere engineering model, Space Sci. Dep., Eur. Space Agency, *ESLAB 87/199*.

Lellouch, E., A. Coustenis, D. Gautier, F. Raulin, N. Dubouloz, and C. Frère (1989), Titan's atmosphere and hypothesized ocean: A reanalysis of the Voyager 1 radio-occcultation and IRIS 7.7 μm data, *Icarus*, *79*, 328–349, doi:10.1016/0019-1035(89)90081-X.

Mahrer, Y., and R. Pielke (1977), A numerical study of airflow over irregular terrain, *Beitr. Phys. Atmos.*, *50*, 98–113.

Niemann, H., et al. (2005), The abundances of constituents of Titan's atmosphere from the GCMS instrument on the Huygens probe, *Nature*, *438*, 779–784, doi:10.1038/nature04122.

Pielke, R., G. Dalu, J. S. T. Lee, and T. Kittel (1992), Nonlinear influence of mesoscale landuse on weather and climate, *J. Clim.*, *4*, 1053–1069.

Pruppacher, H. R., and J. D. Klett (1997), *Microphysics of Clouds and Precipitation*, Springer, New York.

Rafkin, S., R. Haberle, and T. Michaels (2001), The Mars Regional Atmospheric Modeling System: Model description and selected simulations, *Icarus*, *151*, 228–256, doi:10.1006/icar.2001.6605.

Roe, H., I. D. Pater, B. Macintosh, and C. McKay (2002), Titan's clouds from Gemini and Keck adaptive optics imaging, *Astrophys. J.*, *581*, 1399–1406.

Schaller, E., M. Brown, H. Roe, and A. Bouchez (2006), A large cloud outburst at Titan's south pole, *Icarus*, *182*, 224–229, doi:10.1016/j.icarus.2005.12.021.

Thompson, W. R., J. A. Zollweg, and D. H. Gabis (1992), Vapor-liquid equilibrium thermodynamics of N_2 + CH_4: Model and Titan applications, *Icarus*, *97*, 187–199, doi:10.1016/0019-1035(92)90127-S.

Tokano, T., C. McKay, F. Neubauer, S. Atreya, F. Ferri, M. Fulchignoni, and H. Niemann (2006), Methane drizzle on Titan, *Nature*, *442*, 432–435, doi:10.1038/nature04948.

Tomasko, M., et al. (2005), Rain, winds and haze during the Huygens probe's descent to Titan's surface, *Nature*, *438*, 765–778, doi:10.1038/nature04126.

Tremback, C., and R. Kessler (1985), A surface temperature and moisture parameterization for use in mesoscale numerical models, paper presented at Seventh Conference on Numerical Weather Prediction, Am. Meteorol. Soc., Montreal, Que., Canada.

Tripoli, G., and W. Cotton (1982), The Colorado State University three-dimensional cloud/mesoscale model. part I: General theoretical framework and sensitivity experiments, *J. Res. Atmos.*, *16*, 185–220.

E. L. Barth and S. C. Rafkin, Southwest Research Institute, 1050 Walnut Street, Suite 400, Boulder, CO 80302, USA. (ebarth@boulder.swri.edu)